EFFECT OF SERVO SYSTEMS ON THE CONTOURING ERRORS IN INDUSTRIAL ROBOTS

Mohamed Slamani, Albert Nubiola, Ilian A. Bonev
École de technologie supérieure, Montreal (Quebec), Canada
E-mail: ilian.bonev@etsmtl.ca

Received August 2011, Accepted December 2011
No. 11-CSME-75, E.I.C. Accession 3315

ABSTRACT

Two important aspects of the performance of a servo system, tracking errors and contour errors, significantly affect the accuracy of industrial robots under high-speed motion. Careful tuning of the control parameters in a servo system is essential, if the risk of severe structural vibration and a large contouring error is to be avoided. In this paper, we present an overview of a method to diagnose contouring errors caused by the servo control system of an ABB IRB 1600 industrial robot by measuring the robot's motion accuracy in a Cartesian circular shape using a double ballbar (DBB) measurement instrument. Tests were carried out at different TCP (tool centre-point) speed and trajectory radii to investigate the main sources of errors that affect circular contouring accuracy. Results show that radius size errors and out-of-roundness are significant. A simple experimental model based on statistical tests was also developed to represent and predict the radius size error. The model was evaluated by comparing its prediction capability in several experiments. An excellent error prediction capability was observed.

Keywords: robot; accuracy; acontouring error; adynamic error; aservo error; adouble ballbar.

EFFET DES SYSTÈMES ASSERVIS SUR LES ERREURS DE CONTOUR DANS LES ROBOTS INDUSTRIELS

RÉSUMÉ

Les erreurs de poursuite et de contour sont deux aspects importants qui influencent la précision des robots industriels en déplacements rapides. Les paramètres d'un système asservis doivent être soigneusement réglés, car des paramètres non réglés causent souvent des vibrations de structures importantes et une grande erreur de contour. Dans cet article, nous présentons l'aperçu d'une méthode pour diagnostiquer les erreurs de contours dues au système asservi d'un robot industriel ABB IRB 1600, en mesurant la précision des mouvements du robot à partir des trajets circulaires en utilisant l'instrument de mesure « barre à billes ». Des essais ont été effectués à différentes vitesses et à différents rayons de trajectoire pour étudier les principales sources d'erreurs qui affectent la précision de contour circulaire. Les résultats démontrent que les erreurs radiales et les erreurs de circularités sont importantes. Un modèle expérimental simple basé sur des tests statistiques est développé pour représenter et prédire les erreurs radiales. Ensuite, le modèle a été évalué en comparant les prédictions avec des résultats expérimentaux. Une excellente capacité de prédiction a été observée.

Mots-clés : robot; aprécision; aerreurs de contour; aerreurs dynamiques; aerreurs d'asservissement; abarre à billes.

1. INTRODUCTION

Higher speed is a key requirement for productivity enhancement in many automated manufacturing systems. High-accuracy trajectory performance is also a requirement in many industrial robot operations, and should be provided by the servo mechanism. A major problem with the servo systems of industrial robots is contour errors, which occur during curve tracking. A desired curve is the shortest difference between the actual trajectory and that of the reference command. When the robot speed is relatively low, the contour error due to the servo system is usually acceptable. However, once high-speed and high-accuracy are demanded, for example in water jet cutting, laser cutting, gluing, dispensing and deburring, contour errors will have a significant effect [1]. Unfortunately, industrial robots, which were designed to carry out repeatable tasks, are not all that accurate. While robot repeatability ranges typically from 0.02 mm to 0.1 mm, accuracy is often in the order of only a few millimetres [2], and hence the need to improve the performance of contouring control by decreasing or eliminating contour errors as much as possible. There are two common methods for achieving this. One is to design advanced controllers, and the other is path pre-compensation.

In circular contouring, errors can be divided into two categories: out-of-roundness errors (form errors); and radius size errors (size errors). On the robot side, out-of-roundness errors can originate from three major sources: geometric errors, dynamic errors and friction. Geometric errors are usually caused by mechanical or geometrical imperfections, such as link parameter errors, flexibility and wearing of the robot's structural elements [3]. Dynamic errors generally manifest as overshooting, rounding-off and vibration [4]. In the case of vibration, a well-planned trajectory guarantees good path tracking and generates less excitement of the robot's mechanical structure and servo control system, and so this source of error can be avoided [5]. Friction is one of the major limitations in performing high precision manipulation tasks, as it affects both static and dynamic contouring performances, and may cause instability when coupled to position or force feedback control [6].

Radius size error, which can be present at low speeds due to geometric error, is also present at high velocities as a dynamic error (tracking error) caused by the servo control system [1]. For high speed machine tool, it has been observed that the radius size error can reach as much as several hundred micrometers [7] and is proportional to the square of the feedrate and inversely proportional to the curvature radius [8, 9].

Today, the telescopic ballbar is the most common metrology tool for assessing and calibrating the accuracy (the XYZ part) of CMMs and machine tools, and is very popular for calibrating parallel robots [10]. However, its use in industrial serial robots, though proposed more than two decades ago [11], remains very limited (for example, it was used in [12], but in combination with an inclinometer, and in [13] with a reference angular encoder to characterise a six-axis serial robot). In fact, the software that comes with the popular telescopic bar manufactured by Renishaw was specifically developed for use on a machine in which the circular motion is generated by the simultaneous movement of two orthogonal linear axes, and requires that a defined test sequence be followed. The use of the telescopic ballbar in five-axis machine tools, when several axes are driven simultaneously or when rotary axes are driven, is still a subject of research [14,15].

In order to improve the robot's accuracy and efficiency, researchers are looking for ways to measure errors and identify their causes. In this paper, we used the Renishaw QC20-W telescoping ballbar (also called, double ballbar, or DBB) for measuring the contouring performance of a non-calibrated ABB IRB 1600 industrial serial robot. We then analyzed the

data collected and derived an empirical model of radius size error which we validated experimentally.

2. MODELLING APPROACH

Suppose that we have observed data for the radius size error, ΔR, at different TCP speeds for n cases, and would like to determine an empirical model for predicting those errors with two independent variables (X_1 and X_2) that are TCP speed-dependent.

The proposed empirical model can be written as:

$$\Delta R_i = \beta_0 + \beta_1 X_{1_i} + \beta_2 X_{2_i} + \varepsilon_i. \tag{1}$$

Expressing Eq. (1) in matrix form, we have

$$\Delta \mathbf{r} = \mathbf{J}\boldsymbol{\beta} + \boldsymbol{\varepsilon}, \tag{2}$$

where $\Delta \mathbf{r}$ is the n-dimensional column vector of n observations, $\mathbf{J}$ is the $n \times 3$ matrix of independent variables, $\boldsymbol{\beta}$ is the 3-dimensional column vector of parameters, and $\boldsymbol{\varepsilon}$ is the n-dimensional column vector of residual terms.

In least-squares estimation, the sum of the squares of the residual vector elements is minimised. The minimisation is equivalent to:

$$\hat{\beta} = (\mathbf{J}^{\mathbf{T}}\mathbf{J})^{-1}\mathbf{J}^{\mathbf{T}}\Delta \mathbf{r}, \tag{3}$$

provided that the inverse of $\mathbf{J}^{\mathbf{T}}\mathbf{J}$ exists.

Subsequently, a stepwise regression is used to evaluate the marginal contribution of the variables X_1 and X_2. In stepwise regression, terms are kept or removed from the model based on the partial F value. The process begins by including in the model the independent variable having the highest simple correlation with the dependent variable ΔR, i.e. the highest F_j value, on condition that F_j is equal to or exceeds the critical $F_{\alpha;p;n-p}$ value ($F_j \geq F_{\alpha;p;n-p}$), where n is the number of observations, p is the number of estimated parameters and α is the level of significance. If F_j is less than $F_{\alpha;p;n-p}$, the process terminates with no independent variables included in the model.

The F_j value can be calculated by the following equation [14]:

$$F_j = \frac{MSM(X_j)}{MSE(X_j)}, j = 1, \ldots, p, \tag{4}$$

where

$$MSM = \frac{SSR}{p}, \tag{5}$$

$$MSE = \frac{SSE}{n-p}, \tag{6}$$

$$SSE = \sum_{i=1}^{n} (\Delta R_i - \Delta \hat{R}_i)^2, \tag{7}$$

$$SST = \sum_{i=1}^{n} (\Delta R_i - \Delta \overline{R})^2, \tag{8}$$

$$\mathrm{SSR} = \mathrm{SST} - \mathrm{SSE}, \tag{9}$$

$$SSR = \sum_{i=1}^{n} (\Delta \hat{R}_i - \Delta \bar{R})^2, \tag{10}$$

and $\Delta \hat{R}_i$ is the estimated radius size error, $\Delta \bar{R}$ is the mean radius size error, *MSM* is the mean squares model (mean squares due to regression), *MSE* is the mean square error, *SSE* is the sum of squares error, *SST* is the total variation or the total sum of the squares and *SSR* is the explained variation or sum of squares due to regression.

Once the first independent variable is included in the model, the contribution of the second independent variable is determined for the model that already includes the first variable (say X_1). The partial *F* ratio in this case can be calculated by the following equation:

$$F_{2/1} = \frac{MSM(X_2|X_1)}{MSE(X_2,X_1)}. \tag{11}$$

If $F_{2/1}$ is equal to or exceeds the critical value of $F_{\alpha;p;n-p}$, the independent variable is included in the model, otherwise the process terminates.

In stepwise regression, we can also test whether or not the independent variable introduced into the model at an earlier stage may subsequently be removed, once other independent variables have been evaluated.

3. TEST METHODS

Tests were performed on an ABB IRB 1600–6/1.45 industrial robot installed in a laboratory facility with a relatively constant ambient temperature of 21 °C. The robot was manufactured in 2008 and has never been in a collision accident. It does not have either the Absolute Accuracy option (i.e. it is not calibrated) or the Advanced Shape Tuning option (for compensating for the effects of friction at low speeds). A multi-purpose end-effector (readily visible in Fig. 1) was used, onto which the tool cup of the telescoping ballbar is mounted.

Fig. 1. Telescoping ballbar setup for measuring radial errors along a horizontal circular path of radius 300 mm.

The measurement instrument used in this study is a QC20-W telescopic ballbar by Renishaw with Bluetooth wireless technology. It consists of a wireless telescoping ballbar, ballbar extensions, a tool cup, two measuring balls and a pivot assembly. The tool cup is mounted on the robot end-effector. The base of the pivot assembly is magnetic, and is solidly attached to a heavy steel table, as shown in Fig. 1. The ballbar sensor accuracy (at 20 °C) is ± 0.5 µm, and the measuring range is a mere ± 1.0 mm (which is probably too small for large, non-calibrated industrial robots).

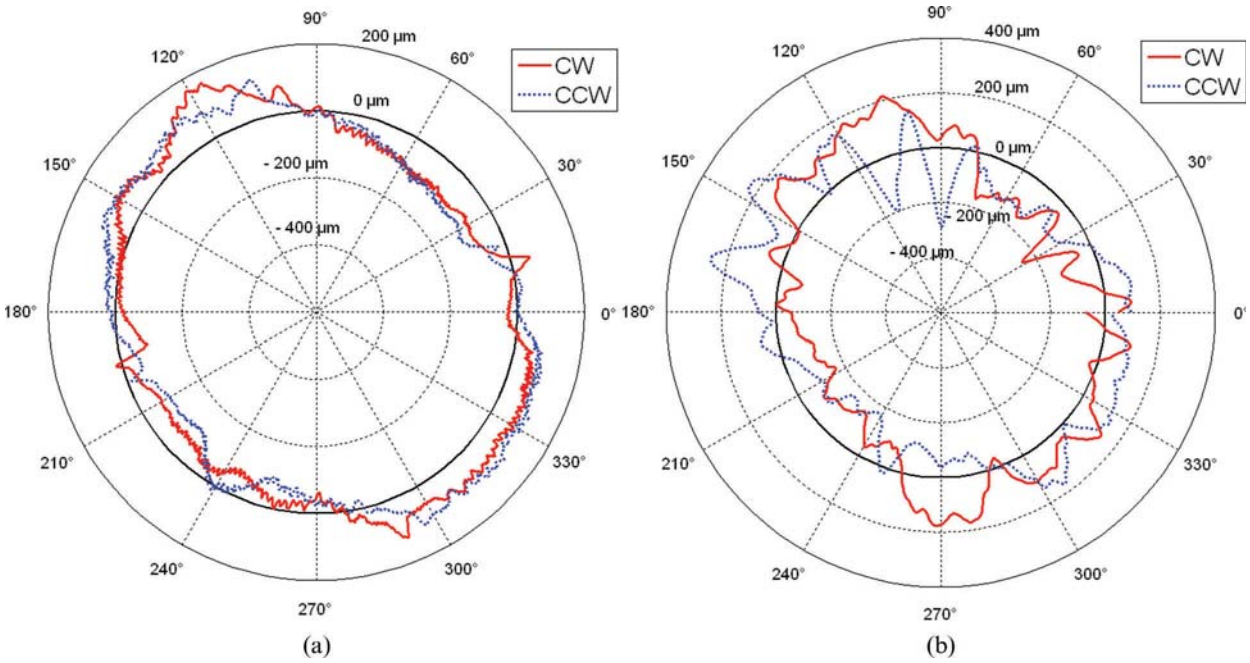

Fig. 2. Steady state contouring form errors in the CW and CWW directions for a horizontal circular path of radius 100 mm centred at approximately {−290 mm, 987 mm, 615 mm}. (a) TCP speed of 30 mm/s. (b) TCP speed of 700 mm/s.

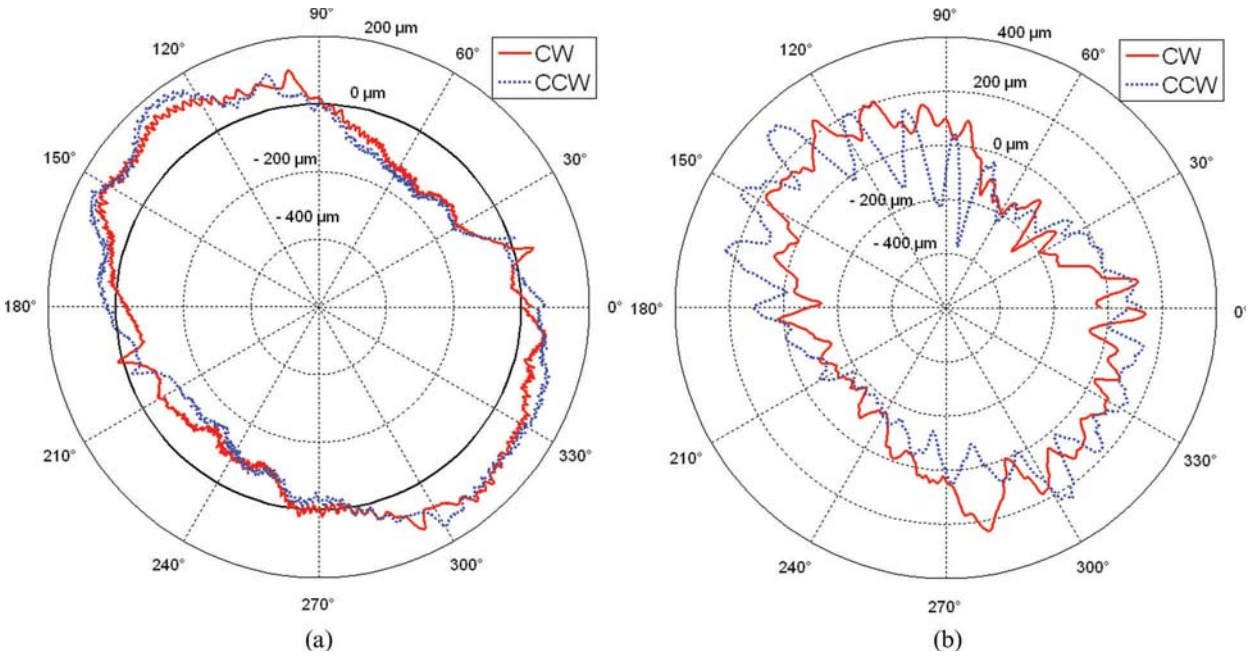

Fig. 3. Steady state contouring form errors in the CW and CWW directions for a horizontal circular path of radius 150 mm centred at approximately {−290 mm, 987 mm, 615 mm}. (a) TCP speed of 30 mm/s. (b) TCP speed of 700 mm/s.

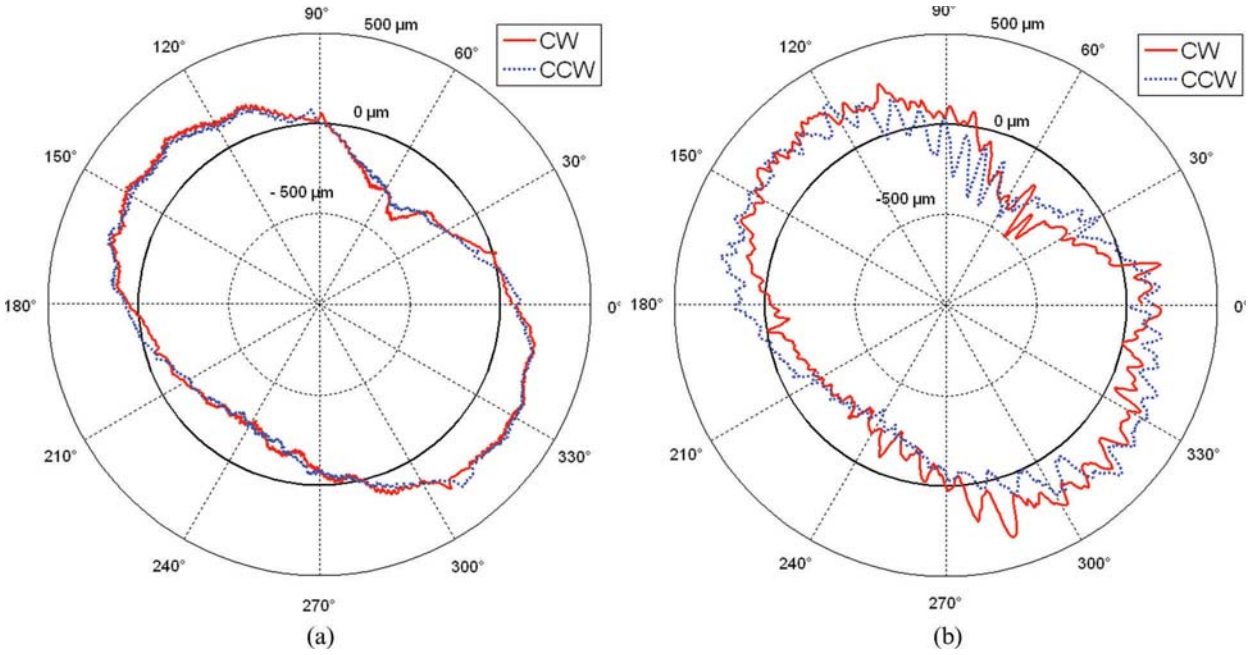

Fig. 4. Steady state contouring form errors in the CW and CWW directions for a horizontal circular path of radius 300 mm centred at approximately {−290 mm, 987 mm, 615 mm}. (a) TCP speed of 30 mm/s. (b) TCP speed of 700 mm/s.

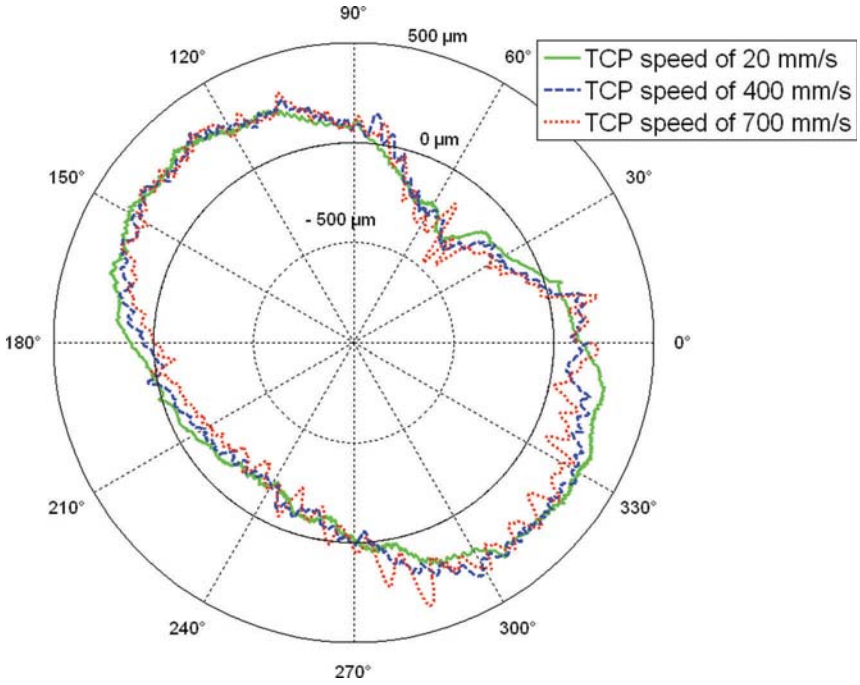

Fig. 5. Steady state contouring form errors in the CW direction for a horizontal circular path of radius of 300 mm and TCP speeds of 20 mm/s, 400 mm/s and 700 mm/s, centred at approximately {−290 mm, 987 mm, 615 mm}.

An end-effector, weighing approximately 2 kg, was used in all the ballbar tests. Circular tests were performed in the clockwise (CW) and counter-clockwise (CCW) directions at radii of 100 mm, 150 mm and 300 mm, and at a constant TCP speed, ranging from 20 mm/s to 700 mm/s. The coordinates of the measurement point (i.e. the centre of the tool cup) with respect to the robot flange reference frame is approximately {0 mm, 65 mm, 149 mm}. To eliminate the effect of not knowing the coordinates of the measurement point precisely, the end-effector is kept at a constant orientation along each circular path.

As the robot runs the ballbar through a sequence of programmed routines, a precision transducer tracks the robot's movement. Renishaw software converts the data into a polar plot of its true movement. Unfortunately, as mentioned above, the ballbar software was developed to analyze CMMs and machine tool data, not robot data. After the end of the test, the raw data are saved and then analysed separately.

As usual, before starting a telescoping bar test, the robot is warmed up by repeating the actual circular trajectory for one hour (from a cold start).

4. DATA ANALYSIS

A circular test with the telescopic ballbar returns a series of measurement values in the [−1 mm, 1 mm] range, approximately. We then add the nominal radius (i.e. the length of the ballbar at which it reads a zero error) to these values to obtain the actual circular path (in a Cartesian reference frame) and fit a least-squares circle, in order to estimate the actual centre of the circular path (which is usually offset by several tens of microns with respect to the taught centre position). A circle of nominal radius is then constructed at the least squares circle centre, and errors are considered with respect to this nominal circle. The *radius size error* is defined as

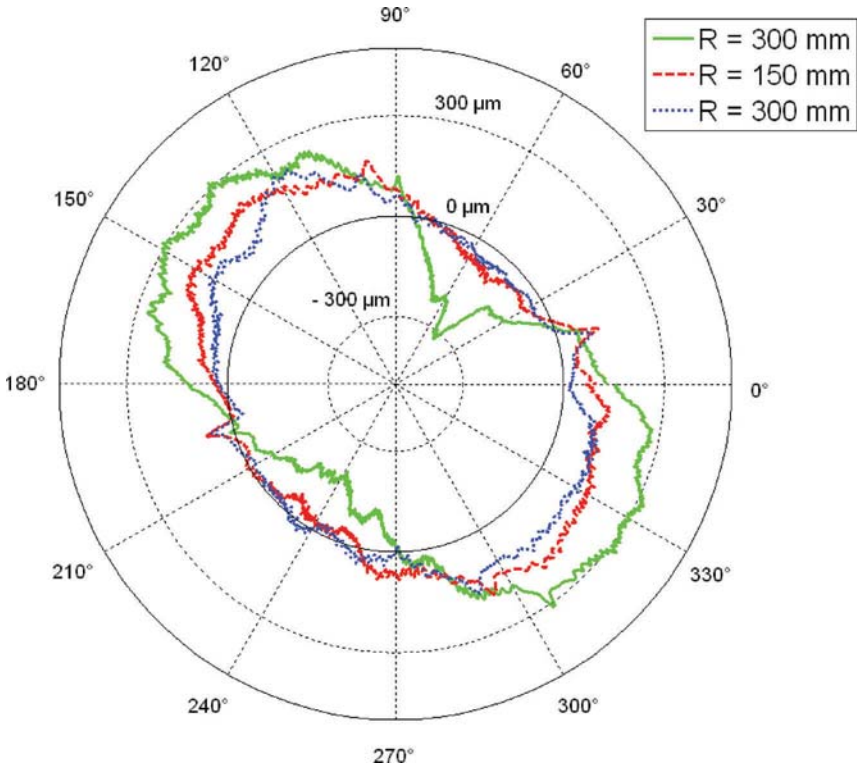

Fig. 6. Steady state contouring form errors in the CW direction for a horizontal circular path of radii 100 mm, 200 mm and 300 mm and at a TCP speed of 20 mm/s,centred at approximately {−290 mm, 987 mm, 615 mm}.

the radius of the least-squares circle minus the nominal radius. *Out-of-roundness* is defined as the difference between the largest and the smallest radial distance from the centre of the least-squares circle to the actual circular path.

Figures 2 to 4 show the steady state contouring form errors with respect to the nominal circle, for both the CW and CCW directions, at TCP speeds of 20 mm/s and 700 mm/s and for nominal radii of 100 mm, 150 mm and 300 mm. The circular paths are centred at approximately {−290 mm, 987 mm, 615 mm} with respect to the robot base reference frame, and lie in a horizontal plane. Figures 2a, 3a and 4a show that the CW and CCW steady state contouring form errors are very similar at low TCP speeds, and significantly different at higher TCP speeds (Figs. 2b, 3b and 4b). Results show also that, in circular paths of large radius, geometric errors are the principal source of errors affecting out-of-roundness, whatever the TCP speed (Figs. 5 and 6). This is revealed by the tilted oval shapes that are clearly visible. In the circular paths of small radius, geometric errors are the principal source of errors affecting out-of-roundness at low TCP speeds (Figs. 6 and 7). At high TCP speeds, dynamic errors become a significant source of errors which affect out-of-roundness (Fig. 7). This is revealed by vibrations along the measured path, which strongly affect the accuracy of the robot (Figs. 2b, 3b, 4b and 7). This behaviour is explained by poor rigidity, as a result flexibility in the joints, which induces vibrations in the end-effector.

It is important to note that the dynamic performance of an industrial robot is even less homogeneous than its static performance. Obviously, the less the main joints (especially joint 1)

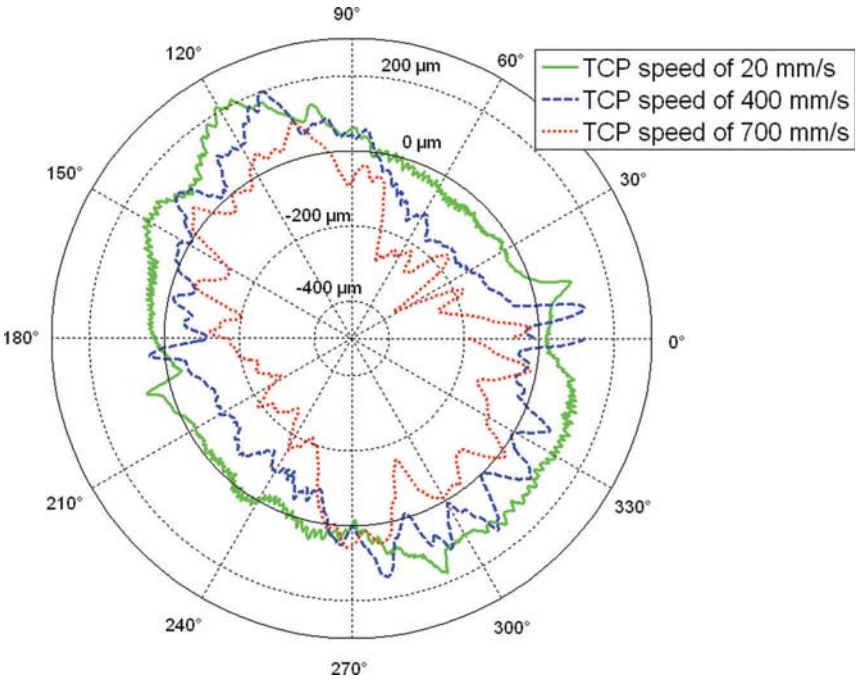

Fig. 7. Steady state contouring form errors in the CW direction for a horizontal circular path of radius of 100 mm and at TCP speedsof 20 mm/s, 400 mm/s and 700 mm/s, centered at approximately {−290 mm, 987 mm, 615 mm}.

are displaced, the better the dynamic performance of the robot. In fact, according to ABB, the best small circular paths are achieved when only two wrist joints are moved.

Figure 8 shows the radius size error for all TCP speeds and nominal radii tested on the robot. Large radius size errors are present at low TCP speeds, due to the effect of geometric errors. The radius size error increases (negatively) with the centripetal acceleration due to dynamic servo

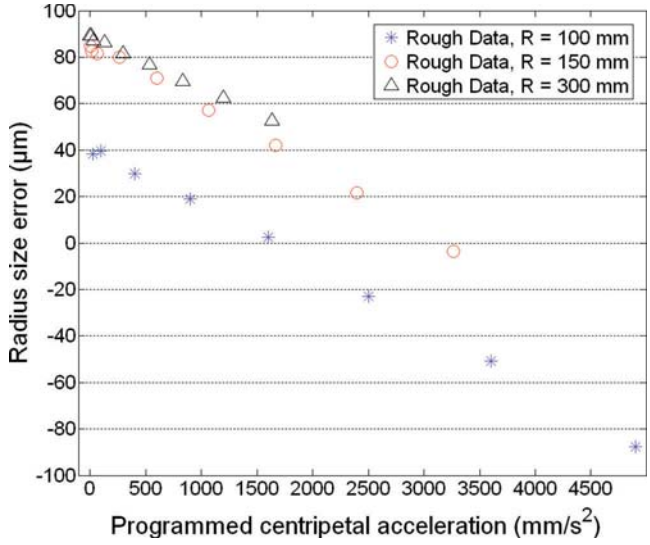

Fig. 8. Radius size error as a function of programmed centripetal acceleration for a horizontal circular path of various radii centred at approximately {−290 mm, 987 mm, 615 mm}.

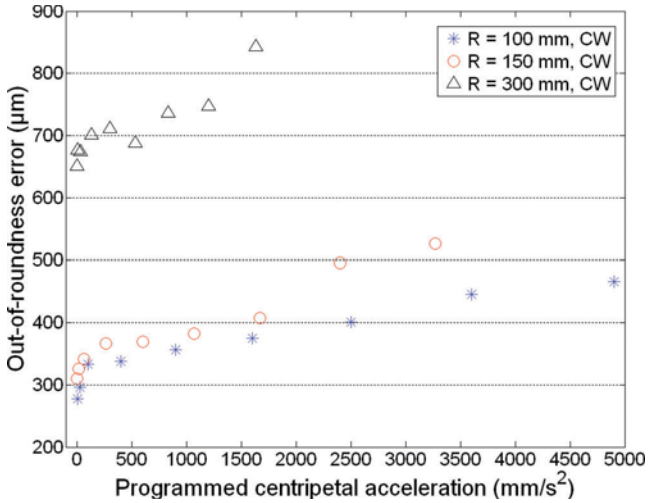

Fig. 9. Out-of-roundness as a function of programmed centripetal acceleration for a horizontal circular path of various radii centred at approximately {−290 mm, 987 mm, 615 mm}.

errors. Similarly, Fig. 9 shows that out-of-roundness increases with centripetal acceleration, owing to the effect of vibrations.

4.1. Derivation of the Empirical Model

According to Chen and Ling [9], the cause of a radius size error for a machine tool is twofold: the servo lag of the servomechanism, and the time delay of the acceleration and deceleration control. They show that, without a feedforward control loop, the radius size error can be expressed as:

$$\Delta R = \frac{1}{2}\left(T^2 + \frac{1}{k_v^2}\right) f^2 / R \tag{12}$$

where R is the radius of the circular test (mm), f is the feedrate (mm/s), k_v is the position gain (1/s) and T is the time constant of the acceleration and deceleration control (s).

Equation (12) shows that the radius size error can be reduced using a smaller time constant of the acceleration and deceleration control (T) and a large position gain (k_v). A similar model is used by Yau et al. for simulating the circular contouring error. In the case of the feedforward axis, the radius size error due to the servo lag can be expressed as [9]:

$$\Delta R = \frac{1}{2}\left(\frac{1 - kf_v^2}{k_v^2}\right) f^2 / R \tag{13}$$

where kf_v is the feedforward factor, which varies between 0 and 1.

Equation (13) shows that the radius size error can be completely eliminated if $kf_v = 1$. The main idea in reducing the radius size error is to keep the response time as short as possible and adjust the feedforward factor. However, this is not an easy task for machine tool users, because sometimes the smaller servo loop response time or larger servo loop gain may cause oscillations or vibrations.

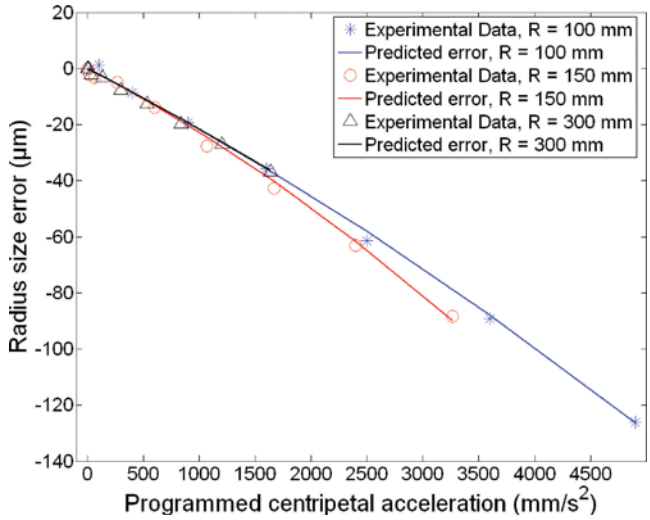

Fig. 10. Experimental and predicted radius size error as a function of the programmed centripetal acceleration for a horizontal circular path of various radii centred at approximately {−290 mm, 987 mm, 615 mm}.

The constant parameters in brackets in Eqs. (12) and (13) become machine tool constants once they have been determined. Since they do not change during machining, Eqs. (12) and (13) can be further rearranged as:

$$\Delta R = K\frac{f^2}{R}. \tag{14}$$

For our industrial robot, our results show that Eq. (14) is not adequate. However, statistical tests show that the servo contouring error for the industrial robot is in good agreement with the following equation:

$$\Delta R = \beta_1\frac{f^2}{R} + \beta_2\frac{f^4}{R^3} \tag{15}$$

where β_1 and β_2 are robot constants, f^2/R is the centripetal acceleration, R is the programmed radius and f is the programmed TCP speed.

Supposing that $X_1 = f^2/R$ and $X_2 = f^4/R^3$, Eq. (15) can be written as follows:

$$\Delta R = \beta_1 X_1 + \beta_2 X_2. \tag{16}$$

We note that β_0 is an offset caused by geometric errors. It represents the radius size error at a low TCP speed and is highly dependent on the radius of the programmed circle. Because we are interested only in the servo error, the measured radius size errors at a TCP speed of 20 mm/s for each radius are removed from the experimental data (Fig. 10). As a result, the offset β_0 tends to zero and is then removed from the model.

4.2. Parameter Estimation and Radius Size Error Prediction

Circular tests at different TCP speeds for radius R = 100 mm are used to estimate the coefficients β_1 and β_2 of Eq. (15). The computed F ratios are F_1 = 1666.5 and F_2 =153.6. The

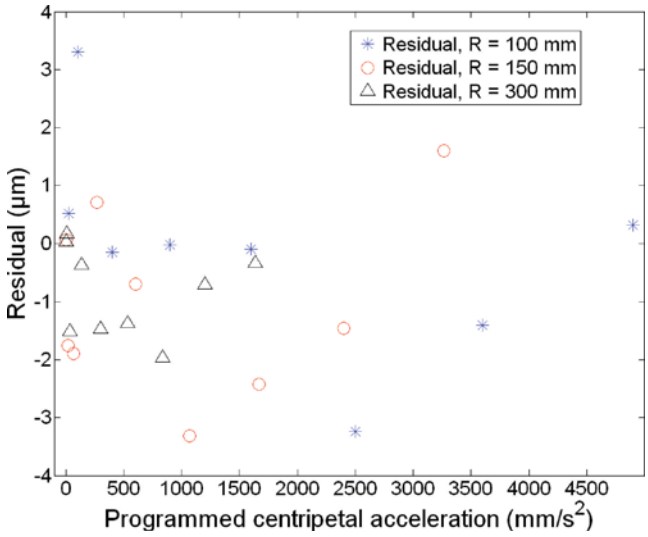

Fig. 11. Residuals between the experimental and predicted radius size error as a function of programmed centripetal acceleration for horizontal circular paths of various radii centred at approximately {−290 mm, 987 mm, 615 mm}.

first independent variable to be included in the model is the variable X_1, because F_1 is larger than F_2 and $F_1 > F_{0.05;1;24} = 4.26$. In the second stage, the contribution of the second independent variable X_2 is determined for the model that already includes the variable X_1. A partial F ratio has to be computed for this variable based on Eq. (17):

$$F_{2,1} = \frac{MSM(X_2|X_1)}{MSE(X_2,X_1)}, \tag{17}$$

where

$$MSM(X_2|X_1) = \frac{SSR(X_2|X_1)}{p}, \tag{18}$$

$$SSR(X_2|X_1) = SSR(X_1,X_2) - SSR(X_1). \tag{19}$$

In the above equations, $SSR(X_1,X_2)$ represents the sum of squares regression when both X_1 and X_2 are included in the model, $SSR(X_2|X_1)$ represents the additional contribution when X_2 is

Table 1. Estimated parameters and the confidence intervals for a 95% confidence level.

Coefficient	Low limit $\times 10^{-3}$	Estimated value $\times 10^{-3}$	High limit $\times 10^{-3}$
β_0(μm)	184.27	1959.27	3734.28
β_1(s^2)	−25.45	−23.29	−21.14
β_2(s^4)	−0.36	−0.23	−0.09

included, given that X_1 is already in the model, and $SSR(X_1)$ represents the contribution when only X_1 is included in the model.

Results show that $F_{2/1} = 21.4$. Since the $F_{2/1}$ value is clearly greater than the critical Fisher value of $F_{0.05;1;24} = 4.26$ at the 0.05 level of significance, then X_2 is included in the model.

To measure the overall quality of the estimation and the uncertainty associated with a specific estimate, a calculation of the confidence region is required. This can be achieved based on Eq. (20). Every estimated value will be in this region, with a confidence level of $100 \times (1-\alpha)\%$ (α being the significance level) [16].

$$\hat{\beta}_j - t_{\frac{\alpha}{2p}-n-p}\sqrt{\sigma^2 C_{jj}} \leq \beta_j \leq \hat{\beta}_j + t_{\frac{\alpha}{2p}-n-p}\sqrt{\sigma^2 C_{jj}} \tag{20}$$

where $\hat{\beta}$ is normally distributed with mean vector $\boldsymbol{\beta}$ and covariance matrix $\sigma^2(\mathbf{J^T J})^{-1}$, C_{jj} is the diagonal element of $(\mathbf{J^T J})^{-1}$, σ^2 is the error variance, n is the number of observations and p is the number of unknowns. The error variance is defined as

$$\sigma^2 = \frac{\Delta \mathbf{r}^T \Delta \mathbf{r} - \hat{\boldsymbol{\beta}}^T \mathbf{J}^T \Delta \mathbf{r}}{n-p}. \tag{21}$$

Table 1 shows the range of values calculated using Eq. (20) for 95% confidence levels.

The estimated coefficients and the statistical model that has been developed are then used to predict the radius size error using experimental data with different radii from those used for identification. As shown in Fig. 10, good agreement was obtained. Furthermore, a closer look at the residuals between the real and predicted radius illustrated in Fig. 11 shows that the model was used successfully to predict the radius size error, as the residuals are smaller than 4 μm.

5. CONCLUSION

Circular tests performed on an ABB IRB 1600-6/1.45 industrial robot show that servo dynamic errors have a significant impact on contouring errors, causing out-of-roundness and potentially large radius size errors. Comparison of the telescoping ballbar tests performed at different TCP speeds shows that the geometric errors are dominant at low TCP speeds and have a significant impact on circular contouring errors. The dynamic errors are present as vibrations, and are dominant at high TCP speeds for small radii, reaching 25% of the total error at a TCP speed of 700 mm/s. Results also show that the tested robot exhibits significant radius size errors. An approach for the modelling and prediction of the radius size error is presented based on experimental data and statistical tests. The developed model was fitted using experimental data, and then its performance was checked by comparing the model predictions to additional sets of data which are different from those used for identification. Results show that the model was able to predict 98% to 99% of the radius size error.

REFERENCES

1. Brogardh, T., "Robot control overview: An industrial perspective," *Modeling, Identification and Control*, Vol. 30, No. 3, pp. 167–180, 2009.

2. Damak, M., Grosbois, J. and De Smet, P., ''Vision robot based absolute accuracy measurement-calibration and uncertainty evaluation,'' *The 35th International Symposium on Robotics*, Paris-Nord Villepinte, France, 2004.
3. Hayati, S., Tso, K. and Roston, G., ''Robot geometry calibration,''*IEEE International Conference on Robotics and Automation*, Philadelphia, PA, USA, Vol. 942, pp. 947–951, 1988.
4. Kataoka, H., Miyazaki, T., Ohishi, K., Katsura, S. and Tungpataratanawong, S., ''Tracking control for industrial robot using notch filtering system with little phase error,'' *Electrical Engineering in Japan*, Vol. 175, No. 1, pp. 793–801, 2011.
5. Olabi, A., Bearee, R., Gibaru, O. and Damak, M., ''Feedrate planning for machining with industrial six-axis robots,'' *Control Engineering Practice*, Vol. 18, No. 5, pp. 471–482, 2010.
6. Lischinsky, P., Canudas-de-Wit, C. and Morel, G., ''Friction Compensation of a Schilling Hydraulic Robot,'' *IEEE International Conference on Control Applications,* Hartford, CT, USA, October 5–7, pp. 294–299, 1997.
7. Slamani, M., Mayer, R., Balazinski, M. and Engin, S., ''Identification and compensation of dynamic scale mismatches in a high-speed end mill boring trajectory on CNC machines,'' *Journal of Manufacturing Science and Engineering*, Vol. 132, No. 3, pp. 0345011–0345016, 2010.
8. Yau, H.T., Ting, J.Y. and Chuang, C.M., ''NC simulation with dynamic errors due to high-speed motion,'' *The International Journal of Advanced Manufacturing Technology*, Vol. 23, No. 7–8, pp. 577–585, 2004.
9. Chen, J.S. and Ling, C.C., ''Improving the machine accuracy through machine tool metrology and error correction,''*International Journal of Advanced Manufacturing Technology*, Vol. 11, No. 3, pp. 198–205, 1996.
10. Ota, H., Shibukawa, T. and Uchiyama, M., ''Forward kinematic calibration method for parallel mechanism using pose data measured by a double ball bar system,'' *Proceedings of the Year 2000 Parallel Kinematic Machines International Conference*, pp. 57–62, 2000.
11. Vira, N. and Lau, K., ''An extensible ball bar for evaluation of robots' positioning performance,'' *Journal of Robotic Systems*, Vol. 4, No. 6, pp. 799–814, 1987.
12. Karlsson, B. and Brogardh, T., ''A new calibration method for industrial robots,'' *Robotica*, Vol. 19, No. 6, 2001.
13. Oh, Y.T., ''Influence of the joint angular characteristics on the accuracy of industrial robots,'' *Industrial Robot: An International Journal*, Vol. 38, No. 4, pp. 406–418, 2011.
14. Lei, W. T., Paung, I. M. and Yu, C.-C. ''Total ballbar dynamic tests for five-axis CNC machine tools,'' *International Journal of Machine Tools & Manufacture*, Vol. 49, No. 6, pp. 488–499, 2009.
15. Zargarbashi, S.H.H. and Mayer, J.R.R. ''Assessment of machine tool trunnion axis motion error, using magnetic double ball bar,'' *International Journal of Machine Tools & Manufacture*, Vol. 46, No. 14, pp. 1823–1834, 2006.
16. Berenson, M.L., Levine, D.M. and Goldstein, M., Intermediate Statistical Methods and Applications: A Computer Package Approach, Prentice-Hall, Englewood Cliffs, 1983.